WIRELESS COMMUNICATIONS AND MOBILE COMPUTING
Wirel. Commun. Mob. Comput. 2015; **15**:2125–2140
Published online 21 May 2014 in Wiley Online Library (wileyonlinelibrary.com). DOI: 10.1002/wcm.2484

RESEARCH ARTICLE

Analytical models for call blocking and dropping in sectorized cellular networks with fractional frequency reuse

Tsang-Ling Sheu, Bo-Jiun Lin and Zi-Tsan Chou*

Department of Electrical Engineering, National Sun Yat-Sen University Kaohsiung, Taiwan

ABSTRACT

In this paper, we construct mathematical models to analyze the probabilities of new call blocking and handoff call (HC) dropping for a sectorized cellular network with fractional frequency reuse (FFR). Because a sectorized FFR network (SFN) consists of two areas, the super group (SG) and the regular group (or sectors), three different types of HCs may happen when a mobile station (MS) moves from the SG to a sector, from a sector to the SG, or from one sector to another sector. To characterize three types of HCs, we first derive the area transition probability, which is defined as the reciprocal of MS's average residence time in an area (i.e., sector or SG). Moreover, we construct the model of Markov chains and derive the state transition rates. Then on the basis of the stationary probabilities of Markovian states, we derive the three types of blocking probabilities of new calls and two types of dropping probabilities of HCs. Finally, we conduct extensive numerical simulations. From the results of numerical simulations, we reveal two important rules for choosing the optimal radius of the SG, with which the system blocking and dropping probability can be effectively minimized. Copyright © 2014 John Wiley & Sons, Ltd.

KEYWORDS

fractional frequency reuse (FFR); sectorized FFR network (SFN); handoff; area transition rate; blocking probability; and Markov chains

***Correspondence**

Zi-Tsan Chou, Department of Electrical Engineering National Sun Yat-Sen University Kaohsiung, Taiwan.
E-mail: ztchou@mail.ee.nsysu.edu.tw

1. INTRODUCTION

Fractional frequency reuse (FFR) techniques [1–3], adopted by Worldwide Interoperability for Microwave Access and long-term evolution-advanced, can effectively increase spectrum utilization by allocating different frequency partitions to different base stations (BSs). A sectorized cellular network with FFR is referred to as a sectorized FFR network (SFN) in this paper. An SFN consists of two regions; each region is employing different kinds of antennas. The inner circle region, employing *omni-directional* antenna, is referred to as the super group (SG). The outer circle region, referred to as the regular group (RG), is further divided into a number of sectors, whereas each sector employs a *unit-directional* antenna.

Previous researches on cellular networks can be divided into three categories. The first category studied cellular networks with omni-directional antenna, the second category studied cellular networks with directional antennas, and the third category studied SFN networks, which employ both omni-directional and directional antennas. For examples, in the first category, V. Goswami *et al.* [4] proposed a channel reservation scheme, which reserves a portion of channels for handoff calls (HCs). If no reserved channels are available, a HC is moved to the first-in-first-out (FIFO) queue. In contrast, in Y. Sun *et al.* [5], a new call will be moved to the FIFO queue if channels are not available. A. Sharma *et al.* [6] divide channels into two groups, high and low-priority ones. A mobile station (MS) with short call holding time basically uses high-priority channels; however, it can employ low-priority channels once all the high-priority channels are used up. Other research works focused on call admission control (CAC). For examples, M. Z. Chowdhury *et al.* [7] considered stringent requirements for real-time traffic. If there is no sufficient channels, the minimum bandwidth for non-real time traffic is reduced. A. Bozkurt *et al.* [8] divide the traffic into two types, voice and data. Their proposed scheme limits the number of voice calls and then computes the allowable amount of data to enter a cellular network. Mobility aware CAC algorithm was proposed by

Y. Kim *et al.* [9]. Unlike the works in [7,8], the authors of [9] define two phases, stop and move, for a HC. In the move phase, a HC is guaranteed to use high-priority channels. Once the handoff is successful, it changes to the stop phase, where a HC uses the low-priority channel as a new call.

In the second category, a cellular coverage is divided into a number of sectors. By considering the overlapping region between two sectors, J. S. Chen *et al.* [10] proposed an allocation algorithm for n sectors with 2^n antenna combinations. C. Mala *et al.* [11] further divide the overlapping region into two regions, high handoff (HHO) and low handoff. To more effectively utilize channels, a genetic algorithm is proposed to predict the moving directions of MSs in HHO. A channel preemption and reservation scheme is proposed by R. Kwan *et al.* [12] for a three-sector cellular network. The proposed scheme combines congestion control and preemptive admission control, which allows high-priority traffic to preempt low-priority traffic under heavy traffic load. H. Shahzad *et al.* [13] proposed an adaptive bandwidth reservation scheme, by which the amount of reserved bandwidth can be computed based on the minimum bandwidth requirement and the probability of handoff. Similarly, M. Al-Sanabani *et al.* [14] combine channel preemption and bandwidth reservation scheme, which allows real-time traffic to preempt channels employed by non-real time traffic. To effectively reduce HC blocking probability, H. Purmehdi *et al.* [15] introduced relays between two neighboring cells.

In the third category, a cellular network with FFR consists of two regions, the SG and the sectors. Most previous works focused on interferences and channel allocations. For example, W. Wang *et al.* [16] proposed service-associated allocation to reduce inter-cell interference. Through simulations, they claimed that their scheme can significantly reduce new call blocking. Cho *et al.* [17] considered co-channel interference (CCI). Their mathematical model analyzes the impact of CCI on the blocking probability of inter-sector and inter-cell HCs. Other researches study how to efficiently allocate and utilize resource blocks (RBs) in the SFN. For example, S. P. Chung *et al.* [18] proposed an RB-borrowing scheme; when no RB is available in the SG, an MS can use RBs belonging to a sector. In contrast, Z. Lu *et al.* [19] allow an MS in a sector to use RBs belonging to the SG. L. Li *et al.* [20] studied the reduction of call blocking if channel borrowing among sectors becomes possible. S. Elayoubi *et al.* [21] considered that it is possible for neighboring cells to use the same frequency. A mathematical model based on Markov chains was built to analyze blocking probability under frequency reuse. Finally, S. Y. Kim *et al.* [22] analyzed call blocking probability for an SFN by using two parameters in Markov chains. The first parameter denotes the channels currently employed in the SG, and the second parameter denotes the channels currently employed in the sectors. However, the authors of [22] did not analyze the performance about HCs.

Unlike the previous work [20–22], in this paper, we construct mathematical models to analyze the new call blocking probability and the HC dropping probability for an SFN with three types of HCs, that is, the HC occurs when an MS moves from the SG to a sector, from a sector to the SG, or from one sector to another sector. To characterize these three types of HCs, we derive the area transition rate of an MS based on the average moving distance and the average moving speed. Markov chains are then built and their state transition rates are formed from the area transition rate of the three types of HCs. By varying the velocity of MS, the number of sectors, and the radius of the SG, we can compute the new call blocking probability and the HC dropping probability. Finally, by numerical simulations, we reveal two rules for choosing the optimal radius of the SG, with which the system blocking and dropping probability can be effectively reduced.

The remainder of this paper is organized as follows. In Section 2, we introduce the architecture of an SFN and the three types of HCs. In Section 3, we build the analytical models of area transition rates and Markov chains, by which we then derive the new call blocking probability and HC dropping probability. In Section 4, numerical simulations are presented and discussed. Finally, conclusions are drawn in Section 5.

2. SECTORIZED FFR NETWORKS

2.1. Super group and sectors in an SFN

Fractional frequency reuse can increase spectrum utilization through frequency reuse technique. Our considered SFN architecture follows the assumptions of [3]. Specifically, an SFN of $N \times S \times K$ represents that, in a cellular network, each cluster contains N cells, each cell consists of S sectors, and each cell employs K frequency partitions. Figure 1(a) demonstrates an example of a $3 \times 3 \times 3$ SFN. Let r and R denote the radius of the SG and the radius of the cell, respectively. We assume that $r < R$. In an SFN, as shown in Figure 1(a), the allocated frequency band, F, to the SG is further partitioned into a number of frequency sub-bands. Each partitioned frequency sub-band is then allocated to a sector such that no adjacent sectors use the same frequency sub-band.

We assume that the physical layer of the SFN is the orthogonal frequency-division multiple access (OFDMA). OFDMA combines the time division multiple access and frequency division multiple access schemes. In an OFDMA system (such as Worldwide Interoperability for Microwave Access), the time domain is segmented into symbols, and each symbol is segmented into (groups of) subcarriers, as shown in Figure 1(b). Moreover, in an OFDMA frame, a symbol and subcarrier combination, referred to as a *block* is the minimum allocable unit. An RB that consists of constant number (H) of blocks is called a *channel* in this paper. We assume that, initially,

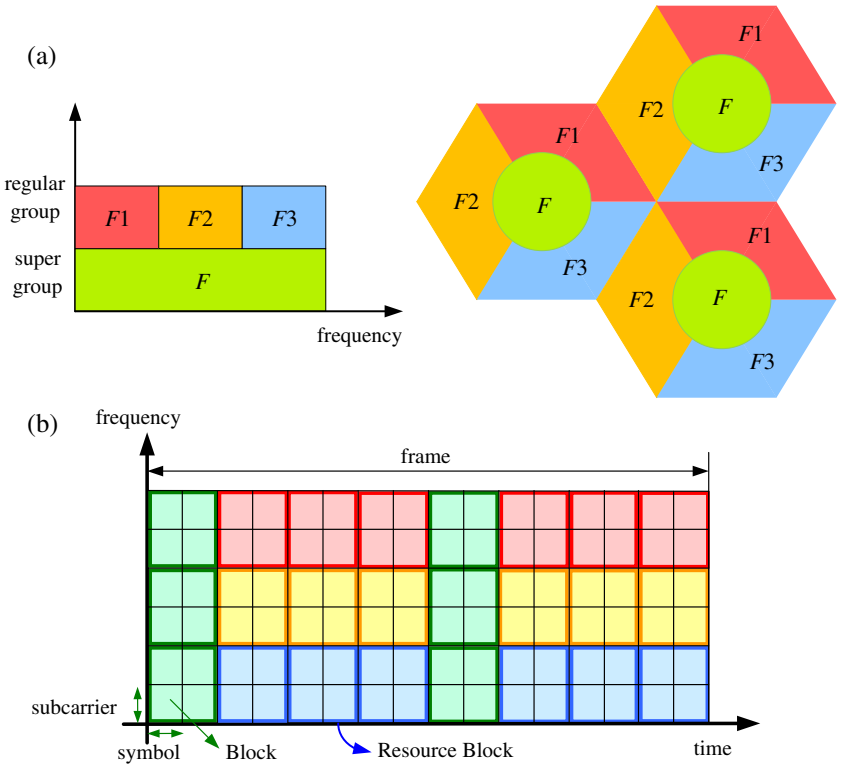

Figure 1. (a) A 3 × 3 × 3 sectorized FFR network (SFN). (b) The concept of channel (resource block) allocation in an OFDMA-based SFN network.

the number of channels allocated to the SG and the RG are based on the ratio of the area of the SG to the area of the RG. Specifically, in an SFN, if there are C_{sg} channels for the SG, and there are C_{sec_i} channels for Sector i, where $1 \leq i \leq n$, we have $C_{\text{sg}} = \frac{r^2}{R^2} C_T$ and $C_{\text{sec}_i} = \left(1 - \frac{r^2}{R^2}\right) \frac{C_T}{n}$, where C_T is the total number of channels in a frame. Figure 1(b) illustrates one possible channel allocation in the SFN where $r = R/2, n = 3, H = 4$, and a frame consists of 16 symbols. Note that in Figure 1(b), $C_T = 24$ and $C_{\text{sg}} = C_{\text{sec}_1} = C_{\text{sec}_2} = C_{\text{sec}_3} = 6$; besides, the channels allocated in frequency band F are colored in green, whereas the channels allocated in $F1, F2$, and $F3$ are colored in red, yellow, and blue, respectively.

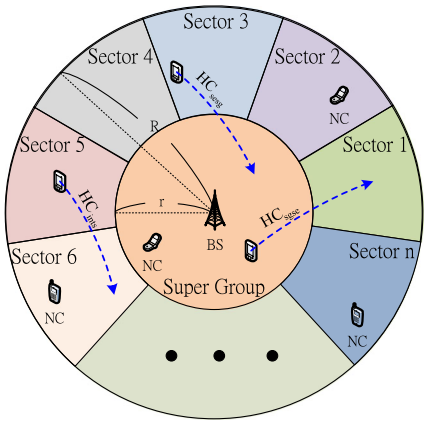

Figure 2. Three types of handoff calls in an SFN.

2.2. Operations of new and handoff calls

This subsection introduces the operations of new calls and HCs. We consider three different types of HCs in an SFN. As shown in Figure 2, the first type is referred to as HC_{sgse}, which happens when an active MS moves from the SG to one of the sectors. Note that an MS is said *active* if the MS's call is ongoing. The second type is referred to as HC_{sesg}, which happens when an active MS moves from one of the sectors to the SG. The third type is referred to as HC_{ints}, which happens when an active MS moves from one sector to another sector.

We assume that each MS requires one channel to establish a call. Figure 3 shows how the BS allocates channels. Note that in Figure 3, $C_{\text{sec}_i}^{avail}$ denotes the number of available channels remaining in sector i, and C_{sg}^{avail} denotes the number of available channels remaining in the SG.

```
BS allocates C_sg channels to the SG and C_sec_i channels to Sector i, for i = 1, 2, …, n.
if MS requests a new call
    if MS is in Sector i
        if C_sec_i^avail > 0
            C_sec_i^avail = C_sec_i^avail − 1;     // A new call is established in Sector i.
        else
            MS's call is blocked;
    else  // MS is in SG
        if C_sg^avail > 0
            C_sg^avail = C_sg^avail − 1;   // A new call is established in the SG.
        else
            MS's call is blocked;
else if MS's call is ongoing
    if MS is in Sector i
        if MS is moving to Sector j   //  j = i + 1 or j = i − 1. An inter-sector HC occurs.
            if C_sec_j^avail > 0
                C_sec_j^avail = C_sec_j^avail − 1;     // MS's call is successfully handed over to Sector j.
                C_sec_i^avail = C_sec_i^avail + 1;     // MS releases its channel to Sector i.
            else
                MS's call is dropped;
        else  // MS is moving to the SG
            if C_sg^avail > 0
                C_sg^avail = C_sg^avail − 1;   // MS's call is successfully handed over to the SG.
                C_sec_i^avail = C_sec_i^avail + 1;     // MS releases its channel to Sector i.
            else
                MS's call is dropped;
    else  // MS is in the SG
        if MS is moving to Sector i
            if C_sec_i^avail > 0
                C_sec_i^avail = C_sec_i^avail − 1;     // MS's call is successfully handed over to Sector i.
                C_sg^avail = C_sg^avail + 1;     // MS releases its channel to the SG.
            else
                MS's call is dropped;
else  // MS's call is terminated.
    if MS is in Sector i
        C_sec_i^avail = C_sec_i^avail + 1;     // MS releases its channel to Sector i.
    else  // MS is in SG
        C_sg^avail = C_sg^avail + 1;     // MS releases its channel to the SG.
```

Figure 3. The operations of new calls and handoff calls in an SFN.

3. MATHEMATICAL MODELS

To simplify the performance analysis, we make the following assumptions. (i) Initially, all MSs are uniformly distributed in a cell. (ii) Each MS first randomly and *independently* selects a direction and then keeps moving according to that direction at the same average moving speed $\overline{v}$. (iii) Once an MS reaches the cell boundary, it repeats the aforementioned mobility behavior. In other words, we focus our analysis on the single cell configuration. Note that, in reality, our assumed mobility model may capture the characteristic of *locality of mobility* [23]. For example, students in the same campus or vehicles on the same roadway may have similar moving speed. The analysis on the multicell configuration is expected to be very complicated and hence left to the future work because it would have to consider intercell HCs from six neighboring cells.

3.1. Area transition rate

The area transition rate (ω) of an MS is defined as the reciprocal of the average residence time ($\overline{T}_{res}$) of an MS in an area (either SG or RG). The average residence time is

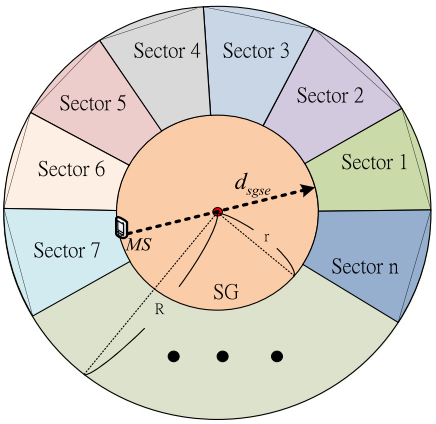

Figure 4. The longest moving distance $\left(d_{sgse}^{\max}\right)$ of an MS that moves from the SG to a sector.

defined as the average moving distance $(\overline{d})$ of an MS in an area divided by the MS's average moving speed $(\overline{v})$, that is, $\overline{T}_{res} = \overline{d}/\overline{v}$. Clearly, the value of $\overline{d}$ depends on the MS's initial location and its moving direction. In what follows, let us consider the following three cases: (i) MS moves from the SG to a sector; (ii) MS moves from a sector to the SG; and (iii) MS moves from one sector to another sector.

(1) Mobile station moves from SG to a sector. In this case, the longest moving distance $\left(d_{sgse}^{\max}\right)$ of an MS that moves from the SG to a sector is $2r$, as shown in Figure 4. On the other hand, the shortest moving distance $\left(d_{sgse}^{\min}\right)$ of an MS that moves from the SG to a sector is 0. Hence, the average residence time $\left(\overline{T}_{res}^{sgse}\right)$ is

$$\overline{T}_{res}^{sgse} = \frac{\left(\frac{d_{sgse}^{\max}+d_{sgse}^{\min}}{2}\right)}{\overline{v}} = \frac{r}{\overline{v}}$$

Next, we assume that the probability of an MS moving from the SG to any one of the sectors is equal. Because we assume that there are n sectors, the area transition rate (from the SG to a sector), which is denoted by ω_{sgse}, is as follows.

$$\omega_{sgse} = \frac{1}{\overline{T}_{res}^{sgse} \times n} \tag{1}$$

(2) Mobile station moves from a sector to the SG. Figure 5 shows the longest moving distance $\left(d_{sesg}^{\max}\right)$ of an MS that moves from a sector to the SG. From Figure 5(a,b), we can observe that the value of $d_{sesg}^{\max}$ depends on the angle, θ_2, which is defined as the angle between edge d_{sesg} and r. From Figure 5(a), we can see that when $\theta_2 = 90°$, we have $d_{sesg}^{\max} = \sqrt{R^2 - r^2}$. On the other hand, when $\theta_2 > 90°$, we have $d_{sesg}^{\max} = \sqrt{R^2 + r^2 - 2rR\cos\left(\frac{2\pi}{n}\right)}$, which can be derived by law of cosines. In fact, the number of sectors, n, can determine the value of θ_2. Specifically, referring to Figure 5, we define $\theta_1 = \frac{2\pi}{n}$ and $\theta_3 = \cos^{-1}\left(\frac{r}{R}\right)$. When $\theta_1 = \theta_3$, we have $\frac{2\pi}{n} = \cos^{-1}\left(\frac{r}{R}\right), \theta_2 = 90°$ and $\sqrt{R^2 - r^2} = \sqrt{R^2 + r^2 - 2rR\cos\left(\frac{2\pi}{n}\right)}$. Because $\theta_1 \geq \theta_3$, we have $\frac{2\pi}{n} \geq \cos^{-1}\left(\frac{r}{R}\right)$. Moreover, if $n \leq \frac{2\pi}{\cos^{-1}\left(\frac{r}{R}\right)}$, we have $d_{sesg}^{\max} = \sqrt{R^2 - r^2}$; otherwise, we have $d_{sesg}^{\max} = \sqrt{R^2 + r^2 - 2rR\cos\left(\frac{2\pi}{n}\right)}$. To sum up the aforementioned discussion, we have the following.

$$d_{sesg}^{\max} = \begin{cases} \sqrt{R^2 - r^2}, & \text{if } n \leq \frac{2\pi}{\cos^{-1}\left(\frac{r}{R}\right)} \\ \sqrt{R^2 + r^2 - 2rR\cos\left(\frac{2\pi}{n}\right)}, & \text{if } n > \frac{2\pi}{\cos^{-1}\left(\frac{r}{R}\right)} \end{cases} \tag{2}$$

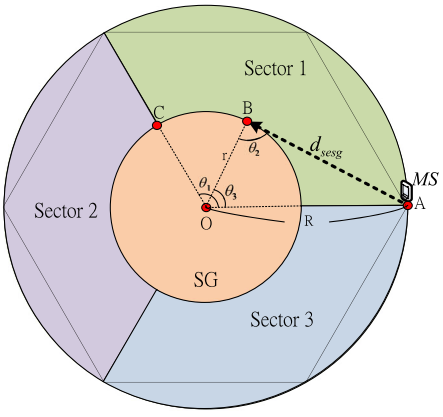

(a) $\theta_2 = 90^0$

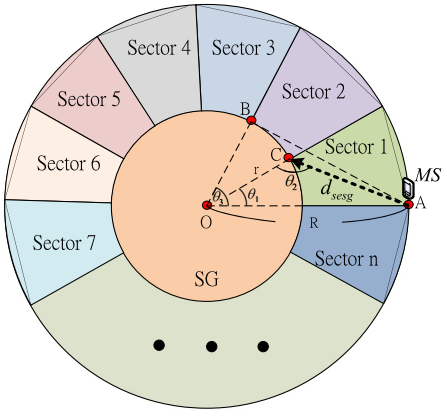

(b) $\theta_2 > 90^0$

Figure 5. The longest moving distance $\left(d_{sesg}^{\max}\right)$ of an MS that moves from a sector to the SG.

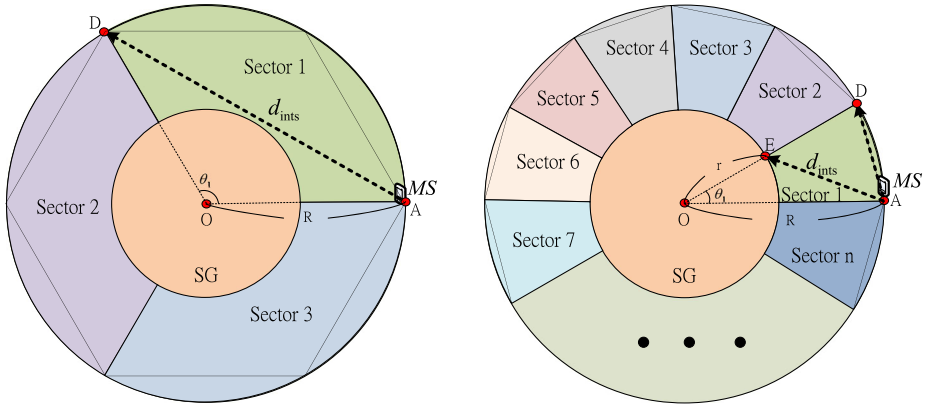

(a) Large sectors (small n) (b) Small sectors (large n)

Figure 6. The longest moving distance $\left(d_{ints}^{\max}\right)$ of an MS that moves from one sector to another.

On the other hand, the shortest moving distance $\left(d_{sesg}^{\min}\right)$ of an MS that moves from a sector to the SG is 0. Thus, the average residence time $\left(\overline{T}_{res}^{sesg}\right)$ and the area transition rate $\left(\omega_{sesg}\right)$ of an MS moving from the SG to a sector can be derived as follows.

$$\overline{T}_{res}^{sesg} = \frac{\left(\frac{d_{sesg}^{\max}+d_{sesg}^{\min}}{2}\right)}{\overline{v}} = \begin{cases} \frac{\sqrt{R^2-r^2}}{2\overline{v}}, & \text{if } n \le \frac{2\pi}{\cos^{-1}\left(\frac{r}{R}\right)} \\ \frac{\sqrt{R^2+r^2-2rR\cos\left(\frac{2\pi}{n}\right)}}{2\overline{v}}, & \text{if } n > \frac{2\pi}{\cos^{-1}\left(\frac{r}{R}\right)} \end{cases} \tag{3}$$

$$\omega_{sesg} = \frac{1}{\overline{T}_{res}^{sesg}} \tag{4}$$

(3) Mobile station moves from one sector to another sector. Figure 5 shows the longest moving distance $\left(d_{ints}^{\max}\right)$ of an MS that moves from one sector to another sector. From Figure 6(a,b), we can observe that the value of $d_{ints}^{\max}$ depends on the angle, θ_1, which is defined as the coverage angle of a directional antenna. As shown in Figure 6(a), when $\theta_1 \ge \frac{2\pi}{n}$, the longest moving distance of an MS that moves from one sector to another sector is equal to the distance from point A to point D. Hence, we have $d_{ints}^{\max} = \overline{AD} = \sqrt{2R^2 - 2R^2\cos\left(\frac{2\pi}{n}\right)}$. On the other hand, as shown in Figure 6(b), when $\theta_1 < \frac{2\pi}{n}$, the longest moving distance of an MS that moves from one sector to another sector is equal to the distance between points A and E. Hence, we have $d_{ints}^{\max} = \overline{AE} = \sqrt{R^2 + r^2 - 2rR\cos\left(\frac{2\pi}{n}\right)}$.

In fact, we can use the number of sectors, n, to determine the value of $d_{ints}^{\max}$. More specifically, when $n = \frac{2\pi}{\cos^{-1}\left(\frac{R+r}{2R}\right)}$, we have $d_{ints}^{\max} = \overline{AD} = \overline{AE}$. Hence, when $n \le \frac{2\pi}{\cos^{-1}\left(\frac{R+r}{2R}\right)}$, we have $d_{ints}^{\max} = \overline{AD}$. On the other hand, the shortest distance $\left(d_{ints}^{\max}\right)$ for an MS moving from one sector to another sector is 0. Thus, the average residence time $\left(\overline{T}_{res}^{\text{ints}}\right)$ and the area transition rate (ω_{ints}) of an MS moving from the SG to a sector can be derived as follows. Note that $\omega_{\text{ints}} = \frac{1}{2\overline{T}_{res}^{\text{ints}}}$ because the probability that an MS moves from a sector to any one of its two adjacent sectors is equal.

$$\overline{T}_{res}^{\text{ints}} = \frac{\left(\frac{d_{ints}^{\max}+d_{ints}^{\min}}{2}\right)}{\overline{v}} = \begin{cases} \frac{\sqrt{2R^2-2R^2\cos\left(\frac{2\pi}{n}\right)}}{2\overline{v}}, & \text{if } n \le \frac{2\pi}{\cos^{-1}\left(\frac{R+r}{2R}\right)} \\ \frac{\sqrt{R^2+r^2-2rR\cos\left(\frac{2\pi}{n}\right)}}{2\overline{v}}, & \text{if } n > \frac{2\pi}{\cos^{-1}\left(\frac{R+r}{2R}\right)} \end{cases} \tag{5}$$

$$\omega_{\text{ints}} = \frac{1}{2\overline{T}_{res}^{\text{ints}}} \tag{6}$$

3.2. Markov chains

We utilize Markov chains to analyze the blocking probability of a new call and the dropping probability of an HC in an SFN. Table I summarizes the parameters used in the following analysis. A Markovian state, $(x_1, x_2, \cdots, x_n, s)$, is defined as a vector of $n+1$ tuples, where the first n tuples individually denote the number of channels currently employed by sector $i (i = 1 \text{ to } n)$, respectively, and the last tuple denotes the channels currently employed by the SG. Clearly, we have $x_1 + x_2 + \ldots + x_n + s \le C_T$. We assume that the generation of new calls follows Poisson distribution with a mean arrival (generation) rate, λ, and the call holding time follows exponential distribution with a mean departure (termination) rate, μ. To simplify our analysis, we assume that the average call holding time

Table I. The longest moving distance ($d_{ints}^{\max}$) of an MS that moves from one sector to another.

r	Radius of the SG
R	Radius of the cell in an SFN
n	Number of Sectors
C_T	Total number of channels initially allocated to an SFN
HC_{sgse}	A handoff call occurring when an MS moves from the SG to a sector
HC_{sesg}	A handoff call occurring when an MS moves from a sector to the SG
HC_{ints}	A handoff call occurring when an MS moves from one sector to another sector
$\overline{T}_{res}^{sgse}$	Average residence time of HC_{sgse}
$\overline{T}_{res}^{sesg}$	Average residence time of HC_{sesg}
$\overline{T}_{res}^{\text{ints}}$	Average residence time of HC_{ints}
ω_{sgse}	Area transition rate of HC_{sgse}
ω_{sesg}	Area transition rate of HC_{sesg}
ω_{ints}	Area transition rate of HC_{ints}
λ	Call arrival (generation) rate
μ	Call departure (termination) rate

MS, mobile station; SG, super group; SFN, sectorized FFR network; HC, handoff call.

$(1/\mu)$ is bounded but sufficiently large. More specifically, we assume that $1/\mu \leq \max\left\{\overline{T}_{res}^{sgse}, \overline{T}_{res}^{sesg}, \overline{T}_{res}^{\text{ints}}\right\}$. Accordingly, for the three types of HCs (i.e., $HC_{\text{sgse}}, HC_{\text{sesg}}$, and HC_{ints}), we can use the area transition rate to define the departure rate of an HC: (i) ω_{sesg}: the departure rate of an HC, which happens when an active MS moves from a sector to the SG; (ii) ω_{sgse}: the departure rate of an HC, which happens when an active MS moves from the SG to a sector; and (iii) ω_{ints}: the departure rate of an HC, which happens when an active MS moves from one sector to another sector. Figure 7 illustrates an example of Markov chain model with three sectors. It is noticed that a Markovian state here has four tuples, (i,j,k,s), where i,j and k denote the number of channels currently employed by sectors 1, 2, and 3, respectively, and s denotes the number of channels currently employed by the SG. Table II shows the arrival and departure processes of the Markov chains. We assume that the three sectors initially allocated the same number of channels, that is, $C_{textsec}$, and the SG allocated C_{sg} channels. Note that, theoretically, $0 \leq x_i \leq C_{\text{sec}}$ and $0 \leq s \leq C_{sg}$. However, in Table II, we use the notations $x_i = C_{\text{sec}b}$ and $s = C_{sgb}$ to represent the situations where MS's call is blocked in sector i and in SG, respectively.

As shown in Figure 7, in our analysis, there are five different types of states in the Markov chains. To come up with the transition matrix for solving the huge-size linear equation, we first need to identify and calculate the number of Markovian states in each type of states. Only after finishing this work, we can obtain the stationary probability of each state to derive the blocking probabilities of new calls and the dropping probabilities of HCs. Table III summaries the conditions of $(x_1, x_2, \ldots, x_n, s)$ for each type of states.

(1) Non-blocking states.
Non-blocking states are the states where at least one channel is available for a new call or an HC. As shown in Figure 7, these states are colored in grey. Refer to Table III because a call will not be blocked even when the value of x_i increases from 0 to C_{sec} and the value of s increases from 0 to C_{sg}, the number of non-blocking states can be computed as follows.

$$N_{nb} = (C_{\text{sec}} + 1)^n \times \left(C_{sg} + 1\right) \tag{7}$$

(2) Blocking states of new calls in the SG.
As shown in Figure 7, these states are colored in blue. A new call generated in the SG is blocked when the SG tries to employ more than C_{sg} channels (i.e., the final tuple, s, reaches the state $s = C_{sgb}$), regardless of the feasible value of x_i. Refer to Table III because the value of x_i ranges from 0 to C_{sec}, the number of blocking states of the new calls in the SG can be computed as follows.

$$N_{sg}^{ncb} = (C_{\text{sec}} + 1)^n \tag{8}$$

(3) Blocking states of new calls in a sector.
As shown in Figure 7, these states are colored in orange. A new call generated in sector i is blocked when sector i tries to employ more than C_{sec} channels (i.e., the tuple, x_i, reaches the state $x_i = C_{\text{sec}\,b}$), regardless of the feasible values of x_j and s, where $i \neq j$. Refer to Table III because the value of x_j ranges from 0 to C_{sec} and the value of s ranges from 0 to C_{sg}, the number of blocking states of the new calls generated in one of the sectors that can be computed as follows.

$$N_{\text{sec}}^{ncb} = (C_{\text{sec}} + 1)^{n-1} \times \left(C_{sg} + 1\right) \times \binom{n}{1} \tag{9}$$

(4) Dropping states of HCs when an active MS moves from a sector to the SG.
An HC is dropped in the SG when an active MS moves into the SG and the number of channels employed in the SG exceeds its maximum. Let $s = (C_{sgb})'$ denote these dropping states. As shown in Figure 7, these states are colored in purple. Note that we use a prime sign outside the parenthesis to distinguish the dropping states from the new call blocking states in SG. Refer to Table III because the states in case 4 cannot occur only when $x_i = C_{\text{sec}}$ for all $1 \leq i \leq n$, the number of dropping states for HCs moving into SG can be computed as follows.

$$N_{sg}^{hcd} = (C_{\text{sec}} + 1)^n - 1 \tag{10}$$

(5) Dropping states of HCs when an active MS moves into a sector.

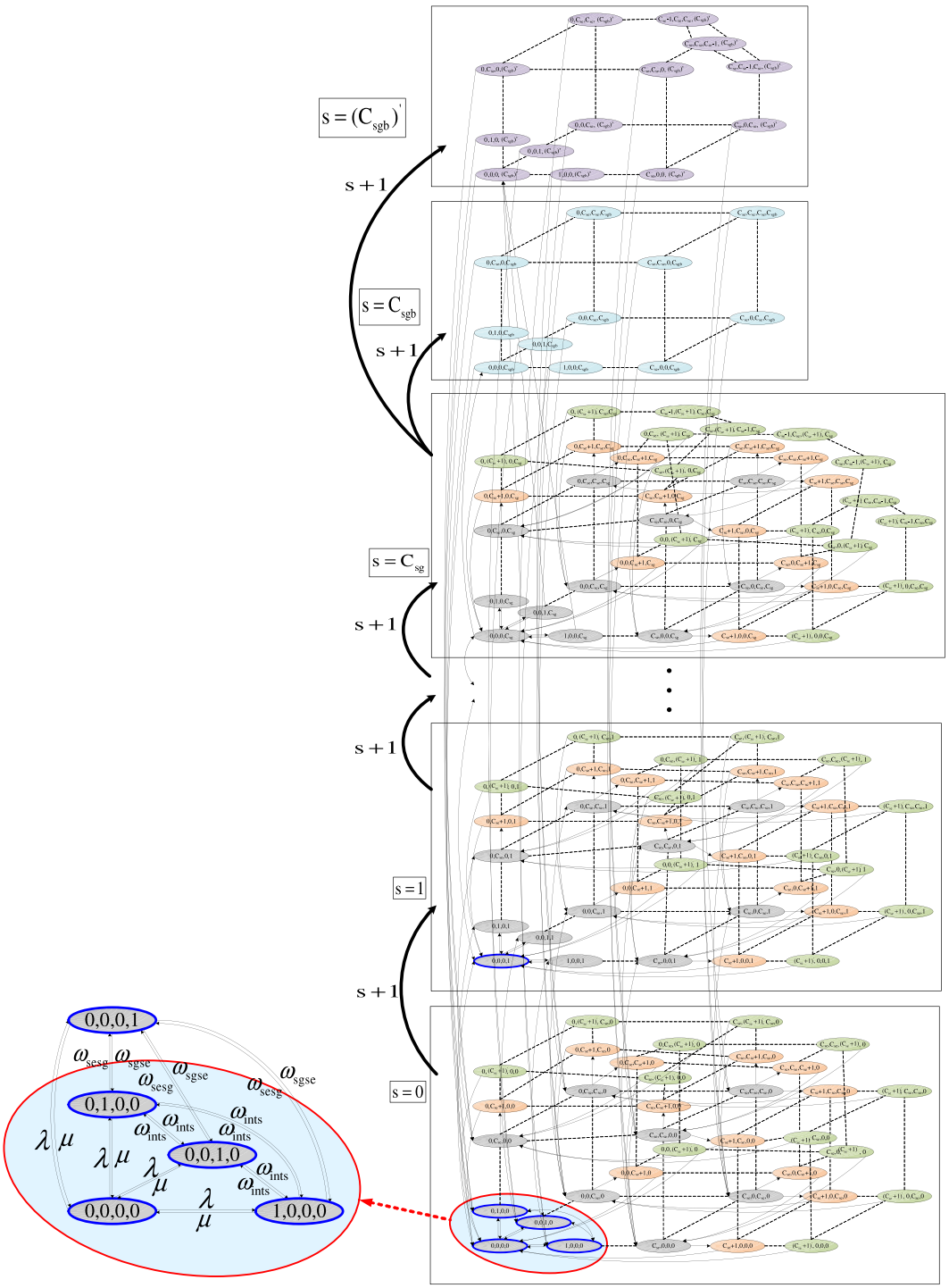

Figure 7. An example of Markov chains with three sectors ($n = 3$).

An HC is dropped in a sector when an active MS moves into Sector i and the number of channels employed in Sector i exceeds its maximum. Let $x_i = (C_{\text{sec}\,b})'$ denote these dropping states. As shown in Figure 7, these states are colored in green. We use a prime sign outside the parenthesis to distinguish the dropping states from the new call blocking states in a sector. Referring to Table III, Equation (11) shows the number of dropping states for HCs moving into a sector. Note that in the right hand side

Table II. State transition rates in Markov chains.

Description	Conditions	State transition rates
	Arrival process	
$(i-1,j,k,s) \rightarrow (i,j,k,s)$	$i \le C_{\text{sec}\,b}$, $j \le C_{\text{sec}}$, $k \le C_{\text{sec}}$, $s \le C_{sg}$	
$(i,j-1,k,s) \rightarrow (i,j,k,s)$	$i \le C_{\text{sec}}$, $j \le C_{\text{sec}\,b}$, $k \le C_{\text{sec}}$, $s \le C_{sg}$	λ
$(i,j,k-1,s) \rightarrow (i,j,k,s)$	$i \le C_{\text{sec}}$, $j \le C_{\text{sec}}$, $k \le C_{\text{sec}\,b}$, $s \le C_{sg}$	
$(i,j,k,s-1) \rightarrow (i,j,k,s)$	$i \le C_{\text{sec}}$, $\le C_{\text{sec}}$, $k \le C_{\text{sec}}$, $s \le C_{sgb}$	
$(i+1,j,k,s) \rightarrow (i,j,k,s)$	$0 \le i < C_{\text{sec}}$, $j \le C_{\text{sec}}$, $k \le C_{\text{sec}}$, $s \le C_{sg}$	$(i+1) \times \mu$
$(i,j+1,k,s) \rightarrow (i,j,k,s)$	$i \le C_{\text{sec}}$, $0 \le j < C_{\text{sec}}$, $k \le C_{\text{sec}}$, $s \le C_{sg}$	$(j+1) \times \mu$
$(i,j,k+1,s) \rightarrow (i,j,k,s)$	$i \le C_{\text{sec}}$, $j \le C_{\text{sec}}$, $0 \le k < C_{\text{sec}}$, $s \le C_{sg}$	$(k+1) \times \mu$
$(i,j,k,s+1) \rightarrow (i,j,k,s)$	$i \le C_{\text{sec}}$, $j \le C_{\text{sec}}$, $k \le C_{\text{sec}}$, $0 \le s < C_{sg}$	$(s+1) \times \mu$
$(i+1,j,k,s-1) \rightarrow (i,j,k,s)$	$0 \le i < C_{\text{sec}}$, $j \le C_{\text{sec}}$, $k \le C_{\text{sec}}$, $s \le C_{sgb}$	$(i+1) \times \omega_{sesg}$
$(i,j+1,k,s-1) \rightarrow (i,j,k,s)$	$i \le C_{\text{sec}}$, $0 \le j < C_{\text{sec}}$, $k \le C_{\text{sec}}$, $s \le C_{sgb}$	$(j+1) \times \omega_{sesg}$
$(i,j,k+1,s-1) \rightarrow (i,j,k,s)$	$i \le C_{\text{sec}}$, $j \le C_{\text{sec}}$, $0 \le k < C_{\text{sec}}$, $s \le C_{sgb}$	$(k+1) \times \omega_{sesg}$
$(i-1,j,k,s+1) \rightarrow (i,j,k,s)$	$i \le C_{\text{sec}\,b}$, $j \le C_{\text{sec}}$, $k \le C_{\text{sec}}$, $0 \le s < C_{sg}$	$(s+1) \times \omega_{sgse}$
$(i,j-1,k,s+1) \rightarrow (i,j,k,s)$	$i \le C_{\text{sec}}$, $j \le C_{\text{sec}\,b}$, $k \le C_{\text{sec}}$, $0 \le s < C_{sg}$	
$(i,j,k-1,s+1) \rightarrow (i,j,k,s)$	$i \le C_{\text{sec}}$, $j \le C_{\text{sec}}$, $k \le C_{\text{sec}\,b}$, $0 \le s < C_{sg}$	
$(i+1,j-1,k,s) \rightarrow (i,j,k,s)$	$0 \le i < C_{\text{sec}}$, $j \le C_{\text{sec}\,b}$, $k \le C_{\text{sec}}$, $s \le C_{sg}$	$(i+1) \times \omega_{\text{ints}}$
$(i+1,j,k-1,s) \rightarrow (i,j,k,s)$	$0 \le i < C_{\text{sec}}$, $j \le C_{\text{sec}}$, $k \le C_{\text{sec}\,b}$, $s \le C_{sg}$	
$(i-1,j+1,k,s) \rightarrow (i,j,k,s)$	$i \le C_{\text{sec}\,b}$, $0 \le j < C_{\text{sec}}$, $k \le C_{\text{sec}}$, $s \le C_{sg}$	$(j+1) \times \omega_{\text{ints}}$
$(i,j+1,k-1,s) \rightarrow (i,j,k,s)$	$i \le C_{\text{sec}}$, $0 \le j < C_{\text{sec}}$, $k \le C_{\text{sec}\,b}$, $s \le C_{sg}$	
$(i-1,j,k+1,s) \rightarrow (i,j,k,s)$	$i \le C_{\text{sec}\,b}$, $j \le C_{\text{sec}}$, $0 \le k < C_{\text{sec}}$, $s \le C_{sg}$	$(k+1) \times \omega_{\text{ints}}$
$(i,j-1,k+1,s) \rightarrow (i,j,k,s)$	$i \le C_{\text{sec}}$, $j \le C_{\text{sec}\,b}$, $0 \le k < C_{\text{sec}}$, $s \le C_{sg}$	
	Departure process	
$(i,j,k,s) \rightarrow (i+1,j,k,s)$		
$(i,j,k,s) \rightarrow (i,j+1,k,s)$	$i \le C_{\text{sec}}$, $j \le C_{\text{sec}}$, $k \le C_{\text{sec}}$, $s \le C_{sg}$	λ
$(i,j,k,s) \rightarrow (i,j,k+1,s)$		
$(i,j,k,s) \rightarrow (i,j,k,s+1)$		
$(i,j,k,s) \rightarrow (i-1,j,k,s)$	$0 < i \le C_{\text{sec}}$, $j \le C_{\text{sec}}$, $k \le C_{\text{sec}}$, $s \le C_{sg}$	$i \times \mu$
$(i,j,k,s) \rightarrow (i,j-1,k,s)$	$i \le C_{\text{sec}}$, $0 < j \le C_{\text{sec}}$, $k \le C_{\text{sec}}$, $s \le C_{sg}$	$j \times \mu$
$(i,j,k,s) \rightarrow (i,j,k-1,s)$	$i \le C_{\text{sec}}$, $j \le C_{\text{sec}}$, $0 < k \le C_{\text{sec}}$, $s \le C_{sg}$	$k \times \mu$
$(i,j,k,s) \rightarrow (i,j,k,s-1)$	$i \le C_{\text{sec}}$, $j \le C_{\text{sec}}$, $k \le C_{\text{sec}}$, $0 < s \le C_{sg}$	$s \times \mu$
$(i,j,k,s) \rightarrow (i-1,j,k,s+1)$	$0 < i \le C_{\text{sec}}$, $j \le C_{\text{sec}}$, $k \le C_{\text{sec}}$, $s \le C_{sg}$	$i \times \omega_{sesg}$
$(i,j,k,s) \rightarrow (i,j-1,k,s+1)$	$i \le C_{\text{sec}}$, $0 < j \le C_{\text{sec}}$, $k \le C_{\text{sec}}$, $s \le C_{sg}$	$j \times \omega_{sesg}$
$(i,j,k,s) \rightarrow (i,j,k-1,s+1)$	$i \le C_{\text{sec}}$, $j \le C_{\text{sec}}$, $0 < k \le C_{\text{sec}}$, $s \le C_{sg}$	$k \times \omega_{sesg}$
$(i,j,k,s) \rightarrow (i+1,j,k,s-1)$		
$(i,j,k,s) \rightarrow (i,j+1,k,s-1)$	$i \le C_{\text{sec}}$, $j \le C_{\text{sec}}$, $k \le C_{\text{sec}}$, $0 < s \le C_{sg}$	$s \times \omega_{sgse}$
$(i,j,k,s) \rightarrow (i,j,k+1,s-1)$		
$(i,j,k,s) \rightarrow (i-1,j+1,k,s)$	$0 < i \le C_{\text{sec}}$, $j \le C_{\text{sec}}$, $k \le C_{\text{sec}}$, $s \le C_{sg}$	$i \times \omega_{\text{ints}}$
$(i,j,k,s) \rightarrow (i-1,j,k+1,s)$		
$(i,j,k,s) \rightarrow (i+1,j-1,k,s)$	$i \le C_{\text{sec}}$, $0 < j \le C_{\text{sec}}$, $k \le C_{\text{sec}}$, $s \le C_{sg}$	$j \times \omega_{\text{ints}}$
$(i,j,k,s) \rightarrow (i,j-1,k+1,s)$		
$(i,j,k,s) \rightarrow (i+1,j,k-1,s)$	$i \le C_{\text{sec}}$, $j \le C_{\text{sec}}$, $0 < k \le C_{\text{sec}}$, $s \le C_{sg}$	$k \times \omega_{\text{ints}}$
$(i,j,k,s) \rightarrow (i,j+1,k-1,s)$		
$(i,j,k,s) \rightarrow (0,j,k,s)$	$i > C_{\text{sec}}$, $j \le C_{\text{sec}}$, $k \le C_{\text{sec}}$, $s \le C_{sg}$	
$(i,j,k,s) \rightarrow (i,0,k,s)$	$i \le C_{\text{sec}}$, $j > C_{\text{sec}}$, $k \le C_{\text{sec}}$, $s \le C_{sg}$	$C_{\text{sec}} \times \mu$
$(i,j,k,s) \rightarrow (i,j,0,s)$	$i \le C_{\text{sec}}$, $j \le C_{\text{sec}}$, $k > C_{\text{sec}}$, $s \le C_{sg}$	
$(i,j,k,s) \rightarrow (i,j,k,0)$	$i \le C_{\text{sec}}$, $j \le C_{\text{sec}}$, $k \le C_{\text{sec}}$, $s > C_{sg}$	$C_{sg} \times \mu$
$(i,j,k,s) \rightarrow (i+1,j,k,s)$		
$(i,j,k,s) \rightarrow (i,j+1,k,s)$	$i \le C_{\text{sec}}$, $j \le C_{\text{sec}}$, $k \le C_{\text{sec}}$, $s \le C_{sg}$	λ
$(i,j,k,s) \rightarrow (i,j,k+1,s)$		
$(i,j,k,s) \rightarrow (i,j,k,s+1)$		
$(i,j,k,s) \rightarrow (i-1,j,k,s)$	$0 < i \le C_{\text{sec}}$, $j \le C_{\text{sec}}$, $k \le C_{\text{sec}}$, $\le C_{sg}$	$i \times \mu$
$(i,j,k,s) \rightarrow (i,j-1,k,s)$	$i \le C_{\text{sec}}$, $0 < j \le C_{\text{sec}}$, $k \le C_{\text{sec}}$, $s \le C_{sg}$	$j \times \mu$
$(i,j,k,s) \rightarrow (i,j,k-1,s)$	$i \le C_{\text{sec}}$, $j \le C_{\text{sec}}$, $0 < k \le C_{\text{sec}}$, $s \le C_{sg}$	$k \times \mu$
$(i,j,k,s) \rightarrow (i,j,k,s-1)$	$i \le C_{\text{sec}}$, $j \le C_{\text{sec}}$, $k \le C_{\text{sec}}$, $0 < s \le C_{sg}$	$s \times \mu$

Table II. *(Continued).*

Description	Conditions	State transition rates
	Departure process	
$(i,j,k,s) \rightarrow (i-1,j,k,s+1)$	$0 < i \leq C_{\text{sec}}$, $j \leq C_{\text{sec}}$, $k \leq C_{\text{sec}}$, $s \leq C_{sg}$	$i \times \omega_{sesg}$
$(i,j,k,s) \rightarrow (i,j-1,k,s+1)$	$i \leq C_{\text{sec}}$, $0 < j \leq C_{\text{sec}}$, $k \leq C_{\text{sec}}$, $s \leq C_{sg}$	$j \times \omega_{sesg}$
$(i,j,k,s) \rightarrow (i,j,k-1,s+1)$	$i \leq C_{\text{sec}}$, $j \leq C_{\text{sec}}$, $0 < k \leq C_{\text{sec}}$, $\leq C_{sg}$	$k \times \omega_{sesg}$
$(i,j,k,s) \rightarrow (i+1,j,k,s-1)$		
$(i,j,k,s) \rightarrow (i,j+1,k,s-1)$	$i \leq C_{\text{sec}}$, $j \leq C_{\text{sec}}$, $k \leq C_{\text{sec}}$, $0 < s \leq C_{sg}$	$s \times \omega_{sgse}$
$(i,j,k,s) \rightarrow (i,j,k+1,s-1)$		
$(i,j,k,s) \rightarrow (i-1,j+1,k,s)$ $(i,j,k,s) \rightarrow (i-1,j,k+1,s)$	$0 < i \leq C_{\text{sec}}$, $j \leq C_{\text{sec}}$, $k \leq C_{\text{sec}}$, $s \leq C_{sg}$	$i \times \omega_{\text{ints}}$
$(i,j,k,s) \rightarrow (i+1,j-1,k,s)$ $(i,j,k,s) \rightarrow (i,j-1,k+1,s)$	$i \leq C_{\text{sec}}$, $0 < j \leq C_{\text{sec}}$, $k \leq C_{\text{sec}}$, $s \leq C_{sg}$	$j \times \omega_{\text{ints}}$
$(i,j,k,s) \rightarrow (i+1,j,k-1,s)$ $(i,j,k,s) \rightarrow (i,j+1,k-1,s)$	$i \leq C_{\text{sec}}$, $j \leq C_{\text{sec}}$, $0 < k \leq C_{\text{sec}}$, $s \leq C_{sg}$	$k \times \omega_{\text{ints}}$
$(i,j,k,s) \rightarrow (0,j,k,s)$	$i > C_{\text{sec}}$, $j \leq C_{\text{sec}}$, $k \leq C_{\text{sec}}$, $s \leq C_{sg}$	
$(i,j,k,s) \rightarrow (i,0,k,s)$	$i \leq C_{\text{sec}}$, $j > C_{\text{sec}}$, $k \leq C_{\text{sec}}$, $s \leq C_{sg}$	$C_{\text{sec}} \times \mu$
$(i,j,k,s) \rightarrow (i,j,0,s)$	$i \leq C_{\text{sec}}$, $j \leq C_{\text{sec}}$, $k > C_{\text{sec}}$, $s \leq C_{sg}$	
$(i,j,k,s) \rightarrow (i,j,k,0)$	$i \leq C_{\text{sec}}$, $j \leq C_{\text{sec}}$, $k \leq C_{\text{sec}}$, $s > C_{sg}$	$C_{sg} \times \mu$

Table III. The conditions for different types of Markovian states. Figure 7 is a special case of Table III where $n = 3$.

Type of states	Conditions of $(x_1, x_2, \ldots, x_n, s)$
1. Non-blocking states	$0 \leq x_i \leq C_{\text{sec}}$, $0 \leq s \leq C_{sg}$
2. Blocking states of new calls in the SG	$0 \leq x_i \leq C_{\text{sec}}$, $s = C_{sgb}$
3. Blocking states of new calls in a sector	$x_i = C_{\text{sec}\,b}$, $0 \leq x_j \leq C_{\text{sec}}\ \forall i \neq j$, $0 \leq s \leq C_{sg}$
4. Dropping states of handoff calls when an active MS moves from a sector to the SG	$s = (C_{sgb})'$, $(x_1, x_2, \ldots, x_n, s) \neq (C_{\text{sec}}, C_{\text{sec}}, \ldots, C_{\text{sec}}, s)$
5. Dropping states of handoff calls when an active MS moves into a sector	$x_i = (C_{\text{sec}\,b})'$, $0 \leq x_j \leq C_{\text{sec}}\ \forall i \neq j$, $0 \leq s \leq C_{sg} - 1$ or $\begin{cases} x_i = (C_{\text{sec}\,b})', 0 \leq x_{i-1} \leq C_{\text{sec}} - 1, 0 \leq x_j \leq C_{\text{sec}}\ \forall j \notin \{i, i-1\}, s = C_{sg} \\ \text{or} \\ x_i = (C_{\text{sec}\,b})', 0 \leq x_{i+1} \leq C_{\text{sec}} - 1, 0 \leq x_j \leq C_{\text{sec}}\ \forall j \notin \{i, i+1\}, s = C_{sg} \end{cases}$

SG, super group; MS, mobile station.

of Equation (11), the first term represents the call-dropping scenario where an active MS moves *from the SG* to a congested sector, under which the value of s ranges from 0 to $C_{sg}-1$, and the second term represents the call-dropping scenarios where an active MS moves *from a sector* to the congested neighboring sector, under which $s = C_{sg}$.

$$N_{\text{sec}}^{hcd} = \left[(C_{\text{sec}} + 1)^{n-1} \times C_{sg} \times \binom{n}{1} \right] + \left[(C_{\text{sec}} + 1)^{n-2} \times \left(2 \times C_{\text{sec}} - (C_{\text{sec}})^2 \right) \times \binom{n}{1} \right] \tag{11}$$

Therefore, the total number of states in Markov chains can be computed by summing up all the five types of states, i.e., $N_{total} = N_{nb} + N_{sg}^{ncb} + N_{\text{sec}}^{ncb} + N_{sg}^{hcd} + N_{\text{sec}}^{hcd}$.

3.3. Blocking and dropping probabilities

By using Markov chains [24], we can derive the stationary probability $\pi(x_1, \cdots, x_n, s)$ of each state $(x_1, \cdots, x_n, s)$. On the basis of stationary probabilities, we show how to derive the new call blocking probability and HC dropping probability in the following. For simplicity, we consider only the case that $n = 3$. Note that other cases ($n \neq 3$) can be derived via the similar ways.

(1) Blocking probability of new calls in the SG
Summing up the stationary probabilities of Markovian states where $s = C_{sgb}$, we have the blocking probability of new calls in the SG (i.e., BP_{sg}), as shown in Equation (12).

$$BP_{sg} = \sum_{x_1=0}^{C_{\text{sec}}} \sum_{x_2=0}^{C_{\text{sec}}} \sum_{x_3=0}^{C_{\text{sec}}} \pi\left(x_1, x_2, x_3, C_{sgb}\right) \tag{12}$$

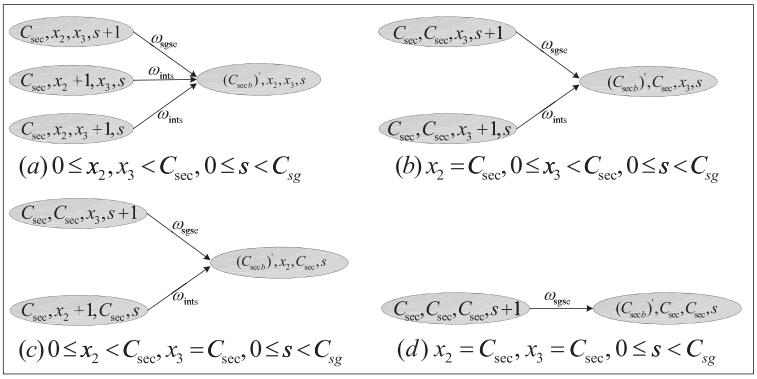

Figure 8. Dropping states of handoff calls when active MSs move from the SG to Sector 1.

(2) Blocking probability of new calls in a sector
Summing up the stationary probabilities of Markovian states where $x_1 = C_{\text{sec}}+1$, we have the blocking probability of new calls in Sector 1 (i.e., BP_{sec}), as shown in Equation (13).

$$BP_{\text{sec}} = \sum_{x_2=0}^{C_{\text{sec}}} \sum_{x_3=0}^{C_{\text{sec}}} \sum_{s=0}^{C_{sg}} \pi\left(C_{\text{sec}\,b}, x_2, x_3, s\right) \quad (13)$$

(3) Dropping probability of HCs from sectors to the SG
Summing up the stationary probabilities of Markovian states where $s = (C_{sgb})'$, we have the dropping probability of HCs from sectors to the SG (i.e., DP_{sesg}), as shown in Equation (14).

$$DP_{sesg} = \sum_{x_1=0}^{C_{\text{sec}}} \sum_{x_2=0}^{C_{\text{sec}}} \sum_{x_3=0}^{C_{\text{sec}}} \pi\left(x_1, x_2, x_3, \left(C_{sgb}\right)'\right) \quad (14)$$

(4) Dropping probability of HCs from the SG to a sector
Let us take Sector 1 as an example. Note that an HC will be dropped when an active MS is in the Markovian states where $x_1 = (C_{\text{sec}\,b})'$ and $s < C_{sg}$. Thus, the dropping probability of HCs from the SG to a sector (i.e., DP_{sgse}) can be computed from Equation (15).

$$DP_{sgse} = \sum_{s=0}^{C_{sg}-1} \left[\sum_{x_2=0}^{C_{\text{sec}}-1} \sum_{x_3=0}^{C_{\text{sec}}-1} \pi\left((C_{\text{sec}\,b})', x_2, x_3, s\right) \times \frac{\omega_{sgse}}{\omega_{sgse} + 2 \times \omega_{\text{ints}}} + \sum_{x_3=0}^{C_{\text{sec}}-1} \pi\left((C_{\text{sec}\,b})', C_{\text{sec}}, x_3, s\right) \times \frac{\omega_{sgse}}{\omega_{sgse} + \omega_{\text{ints}}} + \sum_{x_2=0}^{C_{\text{sec}}-1} \pi\left((C_{\text{sec}\,b})', x_2, C_{\text{sec}}, s\right) \times \frac{\omega_{sgse}}{\omega_{sgse} + \omega_{\text{ints}}} + \pi\left((C_{\text{sec}\,b})', C_{\text{sec}}, C_{\text{sec}}, s\right) \right] \quad (15)$$

Now, we explain the reasons behind each of the four parts in the square brackets of Equation (15). The first part sums the stationary probabilities of states where x_2 and x_3 are all smaller than C_{sec}, as shown in Figure 8(a). Here, because an active MS moving into Sector 1 may come from the SG Sector 2 or Sector 3, we have to multiply the probability by the ratio $\frac{\omega_{sgse}}{\omega_{sgse}+2\omega_{\text{ints}}}$. The second part sums the stationary probabilities of states where x_2 is equal to C_{sec} and x_3 is smaller than C_{sec}, as shown in Figures 8(b). Here, because an active MS moving into Sector 1 may come from the SG or Sector 3, we have to multiply the probability by the ratio $\frac{\omega_{sgse}}{\omega_{sgse}+\omega_{\text{ints}}}$. The third part sums the stationary probabilities of states where x_2 is smaller than C_{sec} and x_3 is equal to C_{sec}, as shown in Figure 8(c). Here, because an active MS moving into Sector 1 may come from SG and Sector 2, we have to multiply the probability by the ratio $\frac{\omega_{sgse}}{\omega_{sgse}+\omega_{\text{ints}}}$. Finally, the last part sums the stationary probabilities of states where x_2 and x_3 are all equal to C_{sec}. Here, an active MS moving into Sector 1 can come from only the SG

(5) Dropping probability of HCs between two neighboring sectors

$$DP_{\text{ints}} = \frac{1}{2} \times \left[\sum_{x_2=0}^{C_{\text{sec}}} \sum_{x_3=0}^{C_{\text{sec}}} \sum_{s=0}^{C_{sg}} \pi\left((C_{\text{sec}\,b})', x_2, x_3, s\right) - DP_{sgse} \right] \quad (16)$$

Let DP_{ints} be the dropping probability of HCs, which occur when active MSs move from one sector to another sector. Let us consider the cases where active

MSs move either from Sector 2 or Sector 3 into Sector 1. The first term in the square brackets of Equation (16) is the dropping probability of HCs (denoted by η), which occur when active MSs move from the SG, Sector 2, or Sector 3 into Sector 1. To obtain the value of η, we need to sum up the probabilities of the states where x_1 is equal to $(C_{\sec b})'$. In Equation (15), we have derived DP_{sgse}, the dropping probability of HCs, which occur when active MSs move from the SG to Sector 1. Thus, the dropping probability of HCs, which occur when active MSs move from Sector 2, or Sector 3 into Sector 1 is $\eta - DP_{sgse}$. Because each sector has two neighboring sectors, we have $DP_{\text{ints}} = \frac{1}{2}\left(\eta - DP_{sgse}\right)$

4. NUMERICAL SIMULATIONS

This section evaluates the new call blocking probability and the three HC dropping probabilities. In the numerical simulations, we fix the transmission range of a BS (i.e., R) to 1000 m. We then vary the MS's average moving speed, the radius of SG, and the number of sectors to observe the impact of these parameters on the system blocking probability. Table IV are the parameters used in our numerical simulations.

4.1. Fixed radius of the SG

Figure 9 shows new call blocking probability in a sector (i.e., $BP_{\sec}$) when the radius of SG is fixed to one half of R. We define the traffic load ρ as the ratio of call arrival rate to call departure rate. From the figure, we can see all curves rise with the increasing of traffic load. Besides, we see that under the condition where the traffic load is 1.2, the value of $BP_{\sec}$ is highest when $n = 6$ and $\overline{v} = 20$ km/hr, whereas the value of $BP_{\sec}$ is lowest when $n = 3$ and $\overline{v} = 100$ km/hr. This is because an active MS with higher moving speed tends to release its channel much faster than an MS with lower moving speed. Further, according to Equations (5) and (6), a larger number of sectors ($n = 6$) will come out with a larger ω_{ints} (the area transition rate of an active MS that moves from one sector to another sector), which will increase the channel contention between HCs and new calls in a sector.

Figure 10 shows new call blocking probability in the SG (i.e., BP_{sg}) when the radius of SG is fixed to 500 m.

Table IV. Parameters and settings.

Parameters	Settings
Radius of an SFN (R)	1000 (m)
The ratio of r and R (i.e., $\alpha = r/R$)	0.25, 0.5, 0.66
Number of sectors (n)	3, 6
Average moving speed of MSs ($\overline{v}$)	20, 100 (km/hr)
Call departure rate (μ)	0.005

SFN, sectorized FFR network.

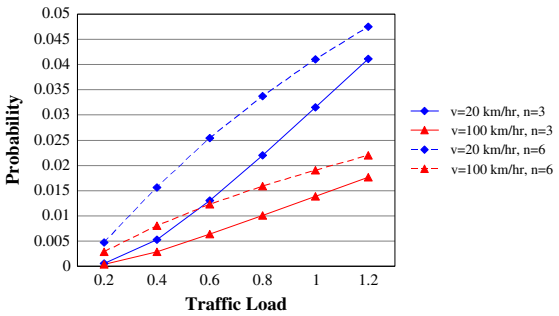

Figure 9. Blocking probability of a new call in a sector.

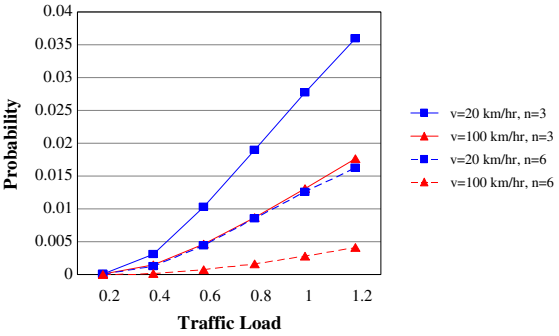

Figure 10. Blocking probability of a new call in the SG.

From Figure 10, we can see that regardless of the vale of n, an active MS with higher moving speed has lower BP_{sg} than an active MS with lower moving speed. However, by comparing Figure 9 with Figure 10, we observe that new call blocking in a sector (i.e., $BP_{\sec}$) is larger than that in the SG (i.e., BP_{sg}). The difference between $BP_{\sec}$ and BP_{sg} becomes even larger when the number of sectors is increased from $n = 3$ to $n = 6$. In other words, Figures 9 and 10 together demonstrate that $BP_{\sec}$ will increase and BP_{sg} will decrease as n is increased. This interesting phenomenon can be explained from two aspects. First, from Figure 9, we can know that new call blocking in a sector ($BP_{\sec}$) will increase as n is increased. Second, from Figure 11(a,b), we can find that when $n = 3$, there are five active MSs moving from a sector to the SG. However, when the value of n becomes 6, two of MS's calls may be dropped (when these two active MSs move into the neighboring sectors) before they move into the SG. Consequently, the channel contention in the SG could be reduced.

By fixing $n = 3$, Figure 12 shows the impact of varying the moving speed of MS on the dropping probability of HCs. HCs occur when active MSs move (i) from the SG to a sector; (ii) from a sector to the SG; or (iii) from one sector to another sector. Note that the dropping probabilities of HCs for these three different moving patterns are denoted by DP_{sgse}, DP_{sesg}, and DP_{ints}, respectively. From the figure, we first observe that regardless of the type of HCs, an active MS with higher moving speed

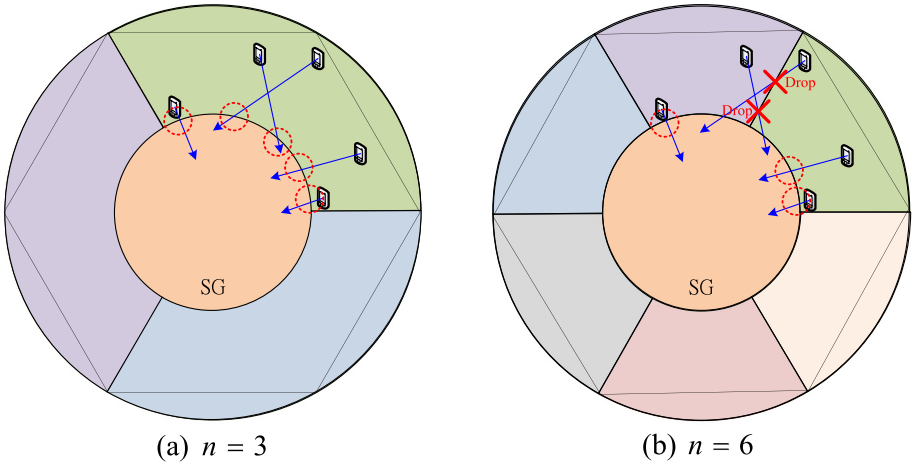

Figure 11. Larger number of sectors may reduce the channel contention in the SG.

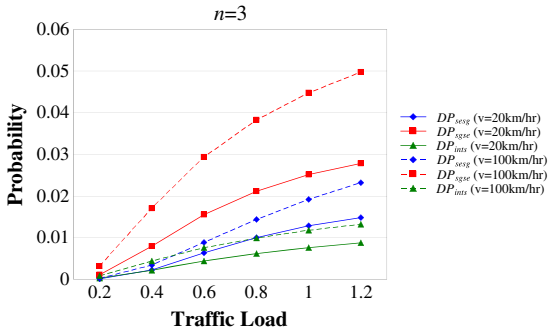

Figure 12. Dropping probability of an HC versus the moving speeds of MSs.

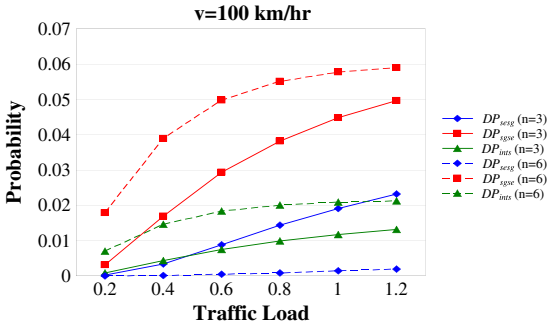

Figure 13. Dropping probability of an HC versus the number of sectors.

(e.g., 100 km/hr) has higher dropping probability than an active MS with lower moving speed (e.g., 20 km/hr). We also observe that among the three dropping probabilities, DP_{sgse} is the highest, DP_{sesg} is the second, and DP_{ints} is the lowest. The reasons are as follows. As shown in Figures 5 and 6, the longest distance for an MS moving from a sector to the SG (i.e., d_{sesg}) is shorter than the longest distance for an MS moving between two sectors (i.e., d_{ints}). Thus, from Equations (4) and (6), we can know that the area transition rate of an MS moving from a sector to the SG (i.e., ω_{sesg}) is higher than that between two sectors (i.e., ω_{ints}). As a result, HCs in the former case occur more often than HCs in the latter case. Hence, DP_{sesg} is higher than DP_{ints}.

Next, we investigate the impact of varying the number of sectors on the dropping probability of an HC. As shown in Figure 13, as the number of sectors is increased from 3 to 6, DP_{sgse} and DP_{ints} increase, whereas DP_{sesg} decreases. The reason for the increase of DP_{sgse} and DP_{ints} is that the value of ω_{ints} increases with the increasing number of sectors. Thus, channel contentions that occur in two types of HCs, HC_{sgse} and HC_{ints}, increase. On the other hand, the reason for the decrease of DP_{sesg} can be explained by Figure 11, which shows that, as the value of n increases, HCs are easier to be dropped in the middle when active MSs move from a sector to the SG.

4.1.1. Adjustable radius of the SG.

By fixing $n = 3$ and $\bar{v} = 100$ km/hr, Figure 14 depicts the impact of changing the radius of SG (r) on the dropping probability of an HC. In the experiments of Figure 14, we set $r = 100, 500$, or 900, where $r = 100$ and $r = 900$ are two close to extreme cases. From Figure 14(a), we observe that DP_{sesg} increases with the increasing value of r. The reason is that as the value of r is increased, the value of $d_{sesg}^{\max}$ (the longest distance of an MS moving from a sector to the SG) becomes smaller, and the value of ω_{sesg} (the area transition rate of an active MS moving from a sector to the SG) becomes larger. To the contrast, Figure 14(b) shows that when the radius of SG is increased, DP_{sgse} becomes smaller as the value of $d_{sgse}^{\max}$ becomes larger. From Figure 14(c), we observe that DP_{ints} becomes much smaller when the radius of SG is increased from 100 to 900 m. The increasing radius of SG definitely reduces the channel contention in a sector because, on average, an active MS requires longer time to move from the SG to a sector to the SG, which in turn decreases ω_{ints} and DP_{ints}.

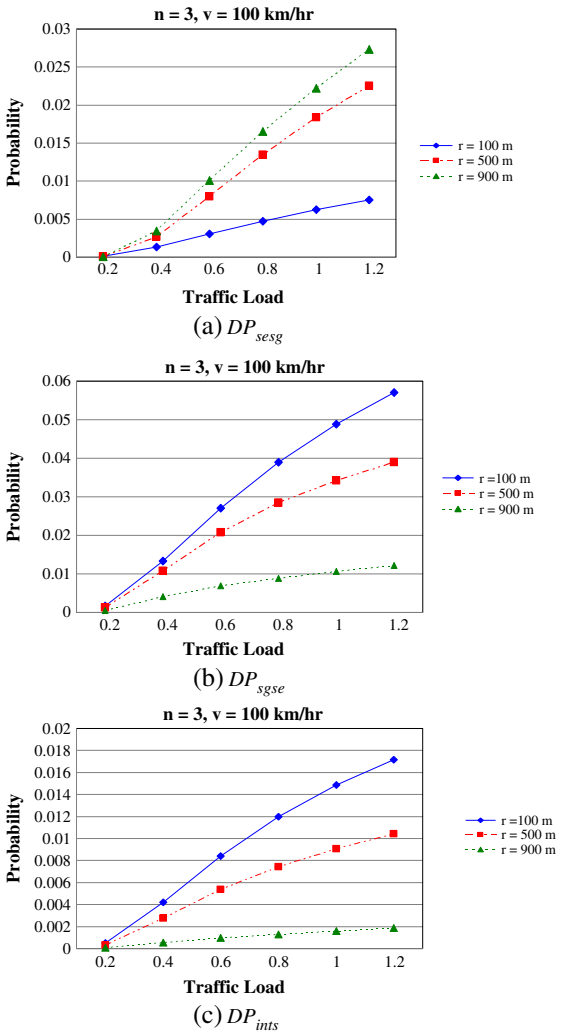

Figure 14. Dropping probability of an HC versus the radius of SG.

Above all, we observe an interesting relationship among three types of dropping probabilities: when the radius of the SG is fixed at 100 m, we have $DP_{sgse} > DP_{\text{ints}} > DP_{sesg}$. However, when the radius of the SG is fixed at 900 m, we have that $DP_{sesg} > DP_{sgse} > DP_{\text{ints}}$.

4.1.2. System blocking and dropping probability.

The optimal radius of the SG (r^*) in an SFN is the value of r with which the sum of new call blocking and HC dropping probabilities can be reduced to the minimum. We define the system blocking and dropping probability (P_{sbd}) as follows.

$$P_{\text{sbd}} = n \times \left(BP_{\text{sec}} + DP_{sesg} + DP_{sgse} + DP_{\text{ints}}\right) + BP_{sg} \tag{17}$$

By fixing traffic load (ρ) to 0.7, Figure 15(a,b) show the system blocking and dropping probability (P_{sbd}) versus the radius of SG, as $\bar{v} = 20$ km/hr and $\bar{v} = 100$ km/hr,

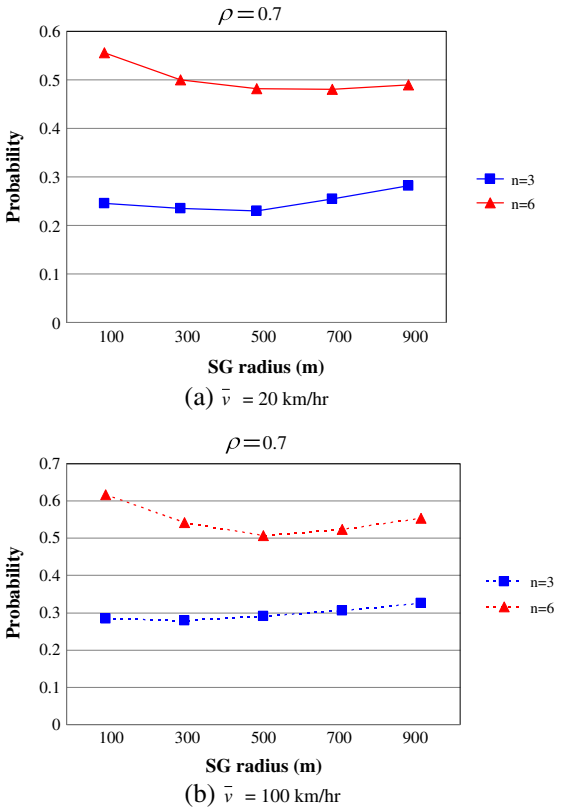

Figure 15. System blocking and dropping probability versus the radius of the SG.

respectively. When $\bar{v} = 20$ km/hr, we observe that P_{sbd} can reach the minimum when $r^* = 0.5R$ if $n = 3$ and $r^* = 0.7R$ if $n = 6$. On the other hand, when $\bar{v} = 100$ km/hr, we observe that P_{sbd} can reach the minimum at $r^* = 0.3R$ if $n = 3$ and $r^* = 0.5R$ if $n = 6$.

Thus, for an SFN, we have discovered two important rules by which a telecom company can reduce the system blocking and dropping probability: (i) for an SFN with a large number of sectors (e.g., $n > 3$), a large radius of the SG is preferred (e.g., $0.5R \leq r^* \leq 0.7R$); and (ii) for an SFN with higher moving speeds of MSs (e.g., $\bar{v} > 20$ Km/h), a small radius of the SG is preferred (e.g., $0.3R \leq r^* \leq 0.5R$).

5. CONCLUSIONS

In this paper, we have presented mathematical models to analyze the new call blocking and the HC dropping probabilities for a sectorized cellular network with FFR. One of the contributions of this paper is to derive the area transition rates of the three types of MS's moving patterns: moving from the SG to a sector, moving from a sector to the SG, and moving from one sector to another sector. Besides, we derived the state transition rates for Markov chains. On the basis of the stationary probabilities

of Markovian states, we have obtained the new call blocking probabilities for the SG and the sectors, respectively. We have also computed the HC dropping probabilities for inter groups and inter sectors. Finally, from the results of numerical simulations, we have suggested two important rules for a telecom company to choose the optimal radius of the SG, with which the system blocking and dropping probability can be effectively minimized.

ACKNOWLEDGEMENTS

The authors would like to thank the editor and the reviewers, whose valuable comments helped improve the presentation of this paper. This work was supported in part by Ministry of Economic Affairs, Taiwan, R.O.C., under grant MOEA 102-EC-17-A-03-S1-214.

REFERENCES

1. Ghaffar R, Knopp R. Fractional Frequency reuse and interference suppression for OFDMA networks. In *International Symposium on Modeling and Optimization in Mobile, Ad Hoc and Wireless Networks (WiOpt)*, Avignon, France, May 31–June 4, 2010; 273–277.
2. Jamal M, Horia B, Maria K, Alexandru I. Study of multiple access cchemes in 3GPP LTE OFDMA vs. SC-FDMA. In *International Conference on Applied Electronics (AE)*, Pilsen, Czech, September 7–8, 2011; 1–4.
3. Xiao H, Feng Z. A novel fractional frequency reuse architecture and interference coordination scheme for multi-cell OFDMA networks. In *IEEE Vehicular Technology Conference (VTC 2010-Spring)*, Taipei, Taiwan, May 16–19, 2010; 1–5.
4. Goswami V, Swain PK. A MAHO based prioritized handoff queueing scheme in cellular networks. In *Third International Conference on Advanced Computing (ICoAC)*, Chennai, India, December 14–16, 2011; 254–259.
5. Sun Y, Li M, Tang LR. A dynamic channel allocation scheme based on handoff reserving and new call queuing. In *International Conference on Control, Automation and Systems Engineering (CASE)*, Singapore, July 30–31, 2011; 1–4.
6. Sharma A, Bhattacharya U. A new channel reservation scheme to reduce call blocking in cellular networks. In *International Conference on Selected Topics in Mobile and Wireless Networking (iCOST)*, Shanghai, China, October 10–12, 2011; 42–47.
7. Chowdhury MZ, Janga YM, Haasb ZJ. Call admission control based on adaptive bandwidth allocation for multi-class services in wireless networks. In *International Conference on Information and Communication Technology Convergence (ICTC)*, Jeju Island, Korea, November 17–19, 2010; 358–361.
8. Bozkurt A, Uçar E, Akdeniz R. Call admission control policy for integration of voice/data traffic in cellular mobile networks. In *Second International Conference on Computational Intelligence,Communication Systems and Networks (CICSyN)*, Liverpool, United Kingdom, July 28–30, 2010; 384–388.
9. Kim Y, Pack S, Lee W. Mobility-aware call admission control algorithm in vehicular WiFi Networks. In *IEEE Global Telecommunications Conference (GLOBECOM 2010)*, Miami, FL, USA, December 6–10, 2010; 1–5.
10. Chen JS, Chen HC, Huang YF, Wei CC, Chuang KC. An adaptive capacity enhancement strategy for sector-based cellular systems. *International Journal on Computers and Mathematics with Applications* 2012; **64**(5): 1462–1472.
11. Mala C, Loganathan M, Gopalan NP, SivaSelvan B. A novel genetic algorithm approach to mobility prediction in wireless networks. In *Second International Conference on Contemporary Computing, Communications in Computer and Information Science,* vol. 40, Noida, India, August 17–19, 2009; 49–57.
12. Kwan R, Arnott R, Trivisonno R, Kubota M. On preemption and congestion control for LTE systems. In *IEEE Vehicular Technology Conference Fall (VTC 2010-Fall)*, Ottawa, Canada, September 6–9, 2010; 1–5.
13. Shahzad H, Taheri H. Resource management based on future traffic estimation and 2-tier structure for 4G cellular network. In *International Conference on Information Technology and e-Services (ICITeS)*, Ottawa, Canada, March 24–26, 2012; 1–4.
14. Al-Sanabani MA, Shamala SK, Othman M, Zukarnain ZA. Multi-class bandwidth reservation scheme based on mobility prediction for handoff in multimedia wireless/mobile cellular networks. *International Journal on Wireless Personal Communications* 2008; **46**(2): 143–163.
15. Purmehdi H, Lahouti F. Channel sharing in hybrid sectorized cellular networks with coverage-limited relays. In *Third UKSim European Symposium on Computer Modeling and Simulation (EMS '09)*, Athens, Greece, November 25–27, 2009; 564–568.
16. Wang W, Xu L, Zhang Y, Zhong J. A novel cell-level resource allocation scheme for OFDMA system. In *International Conference on Communications and Mobile Computing (CMC '09),* vol. 1, Yunnan, China, January 6–8, 2009; 287–292.
17. Cho Y, Oh E, Hong D. A new modeling scenario and analysis of handoff algorithms in multisector sys-

tems with cochannel interference. *IEEE Transactions on Vehicular Technology* 2009; **58**(3): 1407–1414.
18. Chung SP, Chen YW. Performance analysis of call admission control in SFR-based LTE systems. *IEEE Communications Letters* 2012; **16**(7): 1014–1017.
19. Lu Z, Tian H, Sun Q, Huang B, Zheng S. An admission control strategy for soft frequency reuse deployment of LTE systems. In *IEEE Consumer Communications and Networking Conference (CCNC)*, Las Vegas, NV, USA, January 9–12, 2010; 1–5.
20. Li L, Liang D, Wang W. A novel semi-dynamic inter-cell interference coordination scheme based on user grouping. In *IEEE Vehicular Technology Conference Fall (VTC 2009-Fall)*, Anchorage, AK, USA, September 20–23, 2009; 1–5.
21. Elayoubi SE, Haddada OB, Fourestie B. Performance evaluation of frequency planning schemes in OFDMA-based networks. *IEEE Transactions on Wireless Communications* 2008; **7**(5): 1623–1633.
22. Kim SY, Ryu S, Choc CH, Lee HW. Performance analysis of a cellular network using frequency reuse partitioning. *International Journal on Performance Evaluation* 2013; **70**(2): 77–89.
23. Wang W, Zhao M. Joint effects of radio channels and node mobility on link dynamics in wireless networks. In *IEEE INFOCOM*, Phoenix, AZ, USA, 2008; 1606–1614.
24. Nelson R. *Probability, Stochastic Processes, and Queueing Theory*. Springer-Verlag: Inc: New York, USA, 2010.

AUTHORS' BIOGRAPHIES

Tsang-Ling Sheu received the PhD degree in computer engineering from the Department of Electrical and Computer Engineering, Penn State University, University Park, Pennsylvania, USA, in 1989. From September 1989 to July 1995, he worked with IBM Corporation at Research Triangle Park, North Carolina, USA. In August 1995, he became an associate professor and was promoted to full professor in January 2006 at the Department of Electrical Engineering, National Sun Yat-Sen University, Kaohsiung, Taiwan. His research interests include wireless networks, mobile communications, and multimedia networking. He was the recipient of the 1990 IBM outstanding paper award. Dr. Sheu is a senior member of the IEEE and the IEEE Communications Society.

Bo-Jiun Lin received the BS degree from the Department of Applied Mathematics, National Tai-Chung Education University, Tai-Chung, Taiwan, in 2006 and the MS degree from the Department of Electrical Engineering, National Sun Yat-Sen University, Kaohsiung, Taiwan, in 2013. His research interest is in the area of wireless communications and cellular networks, particularly in FFR networks.

Zi-Tsan Chou received the PhD degree in Computer Science and Information Engineering from National Taiwan University. He is currently an assistant professor in the Department of Electrical Engineering, National Sun Yat-Sen University, Kaohsiung, Taiwan. His industrial experience includes NEC Research Institute (America) and Institute for Information Industry (Taiwan). He holds eight United State patents, eleven Taiwan patents, and three China patents in the field of wireless communications. His research interests include medium access control, power management, and quality-of-service control for wireless networks. He is a member of both the IEEE and the IEEE Communications Society.